Precise timing is ubiquitous, consistent, and coordinated across a comprehensive, spike-resolved flight motor program

Joy Putney[a,b,1], Rachel Conn[c,d,1], and Simon Sponberg[a,b,c,2]

[a]School of Biological Sciences, Georgia Institute of Technology, Atlanta, GA 30332; [b]Graduate Program in Quantitative Biosciences, Georgia Institute of Technology, Atlanta, GA 30332; [c]School of Physics, Georgia Institute of Technology, Atlanta, GA 30332; and [d]Neuroscience Program, Emory University, Atlanta, GA 30322

Edited by John G. Hildebrand, University of Arizona, Tucson, AZ, and approved October 4, 2019 (received for review May 1, 2019)

Sequences of action potentials, or spikes, carry information in the number of spikes and their timing. Spike timing codes are critical in many sensory systems, but there is now growing evidence that millisecond-scale changes in timing also carry information in motor brain regions, descending decision-making circuits, and individual motor units. Across all of the many signals that control a behavior, how ubiquitous, consistent, and coordinated are spike timing codes? Assessing these open questions ideally involves recording across the whole motor program with spike-level resolution. To do this, we took advantage of the relatively few motor units controlling the wings of a hawk moth, *Manduca sexta*. We simultaneously recorded nearly every action potential from all major wing muscles and the resulting forces in tethered flight. We found that timing encodes more information about turning behavior than spike count in every motor unit, even though there is sufficient variation in count alone. Flight muscles vary broadly in function as well as in the number and timing of spikes. Nonetheless, each muscle with multiple spikes consistently blends spike timing and count information in a 3:1 ratio. Coding strategies are consistent. Finally, we assess the coordination of muscles using pairwise redundancy measured through interaction information. Surprisingly, not only are all muscle pairs coordinated, but all coordination is accomplished almost exclusively through spike timing, not spike count. Spike timing codes are ubiquitous, consistent, and essential for coordination.

motor control | flight | information theory | spike timing | temporal code

Neurons convey information through not only the number of spikes but also their timing (1–4). In sensory systems, both changes in the number of spikes over time and precise, millisecond-level shifts in sequences of spikes are well established as essential encoding mechanisms for proprioception (5), audition (6), vision (1, 7–9), touch (10), and other modalities (7, 11, 12). Spike timing codes have been shown to be of particular importance in sensory systems (1, 8), and patterns of multiple spikes can convey more information about a stimulus than the sum of the individual timings (13). In vertebrate motor systems, rate codes, where muscle force is proportional to the firing rate of the motor neuron, are thought to predominate, in part due to recruitment principles of many motor units and the presumed low-pass nature of muscles (14–17). Although vertebrate muscle force may be modulated by spike rate under isometric conditions (15), precisely timed patterns of spikes affect the output force of muscle (18). Similarly, in invertebrates, rate codes can adjust force development in muscles, but the absolute number of spikes (spike count code) also matters (19, 20). The onset time of a single spike or burst is also known to play a functional role for the control of invertebrate muscle (21–24).

Recent evidence in invertebrates and vertebrates shows that spike timing codes may be underappreciated for controlling motor behaviors, at least in specific muscles or motor circuits (4). Spike timing codes in which information is encoded in the precise timing patterns of neural or muscular action potentials have an even higher capacity to code for the output of muscles than rate or count (4, 13, 18). Such codes are found in a songbird cortical area for vocalization (25) and in mouse cerebellum for task error correction (26). Correlational, causal, and mechanistic studies show that millisecond-level changes in timing of spikes in motor neurons can manifest profound changes in force production (27) and even behavior selection (28). Causal evidence in support of spike timing codes is present in fast behaviors like invertebrate flight (27), but also in relatively slow behaviors like breathing in birds (18). However, evidence for the importance of spike timing codes in motor systems has been limited to only a few of the motor signals that typically control movement. Whether such timing codes are utilized broadly across a complete motor program for behavior is unknown, as is their role in coordinating multiple motor units. Despite growing appreciation of the potential for motor timing codes, we have not yet established the ubiquity, consistency, and coordination of spiking timing across the motor signals that compose a behavior. This poses 3 hypotheses.

First, timing codes may be restricted to only a few motor signals that control behavior. For example, recordings of muscles in locusts, hawk moths, and fruit flies have shown that spike timing and count variation are prevalent in specific motor units (21, 22, 29). Alternatively, timing codes may be

Significance

Brains can encode precise sensory stimuli, and specific motor systems also appear to be precise, but how important are millisecond changes in timing of neural spikes across the whole motor program for a behavior? We record nearly every spike that the hawk moth's nervous system sends to its wing muscles. We show that all muscles convey the majority of their information in spike timing. The number of spikes does play a role, but not in a coordinated way across muscles. Instead, all coordination is done using the millisecond timing of spikes. The importance and prevalence of timing across the motor program pose questions for how nervous systems create precise, coordinated motor commands.

Author contributions: J.P., R.C., and S.S. designed research, performed research, analyzed data, and wrote the paper.

The authors declare no competing interest.

This article is a PNAS Direct Submission.

[1]J.P. and R.C. contributed equally to this work.

[2]To whom correspondence may be addressed. Email: sponberg@gatech.edu.

This article contains supporting information online at https://www.pnas.org/lookup/suppl/doi:10.1073/pnas.1907513116/-/DCSupplemental.

First published December 16, 2019.

ubiquitous—widespread across the entire motor program and present in all muscles controlling a behavior.

Regardless of the prevalence of timing codes, motor neurons within the population may exhibit specialized encoding strategies, varying the amount of information transmitted through spike timing or spike count depending on the function of the muscles they innervate. For example, *Drosophila* use combinations of functionally distinct phasic and tonic motor units to control flight (23). Additionally, evidence in some sensory systems shows that separate classes of neurons use either spike rate or spike timing to convey information (30). Alternatively, the entire motor program may be consistent in its use of spike timing for encoding.

Finally, coordination of multiple motor signals is typically assessed through covariation in firing rates. For example, motor coordination patterns across muscles [e.g. muscle synergies (31)] and population recordings of M1 neurons in motor cortex (32) all consider how populations of units encode movement through spike rate. Alternatively, spike timing codes may play a role in the coordination of muscles in motor systems. Resolving these hypotheses about the role of spike timing in motor control is challenging because they consider encoding strategies across an entire motor program. It is therefore necessary to record from a spike-resolved, comprehensive set of signals that control a behavior simultaneously in a consistent behavioral context.

Recording such a comprehensive motor program is difficult due to the requirements of completeness, sufficient temporal resolution, and sampling rich variation in a naturalistic behavior. Obtaining a nearly complete motor program is more tractable in the peripheral nervous system than in central regions, because of smaller neuronal population sizes. While many muscles or motor units have been simultaneously recorded using electromyography (EMG) in frogs (33), cats (31), and humans (34) and using calcium imaging in the wing steering muscles of fruit flies (23), these sets of neural signals are not spike-resolved. Large flying insects are feasible organisms in which to record a

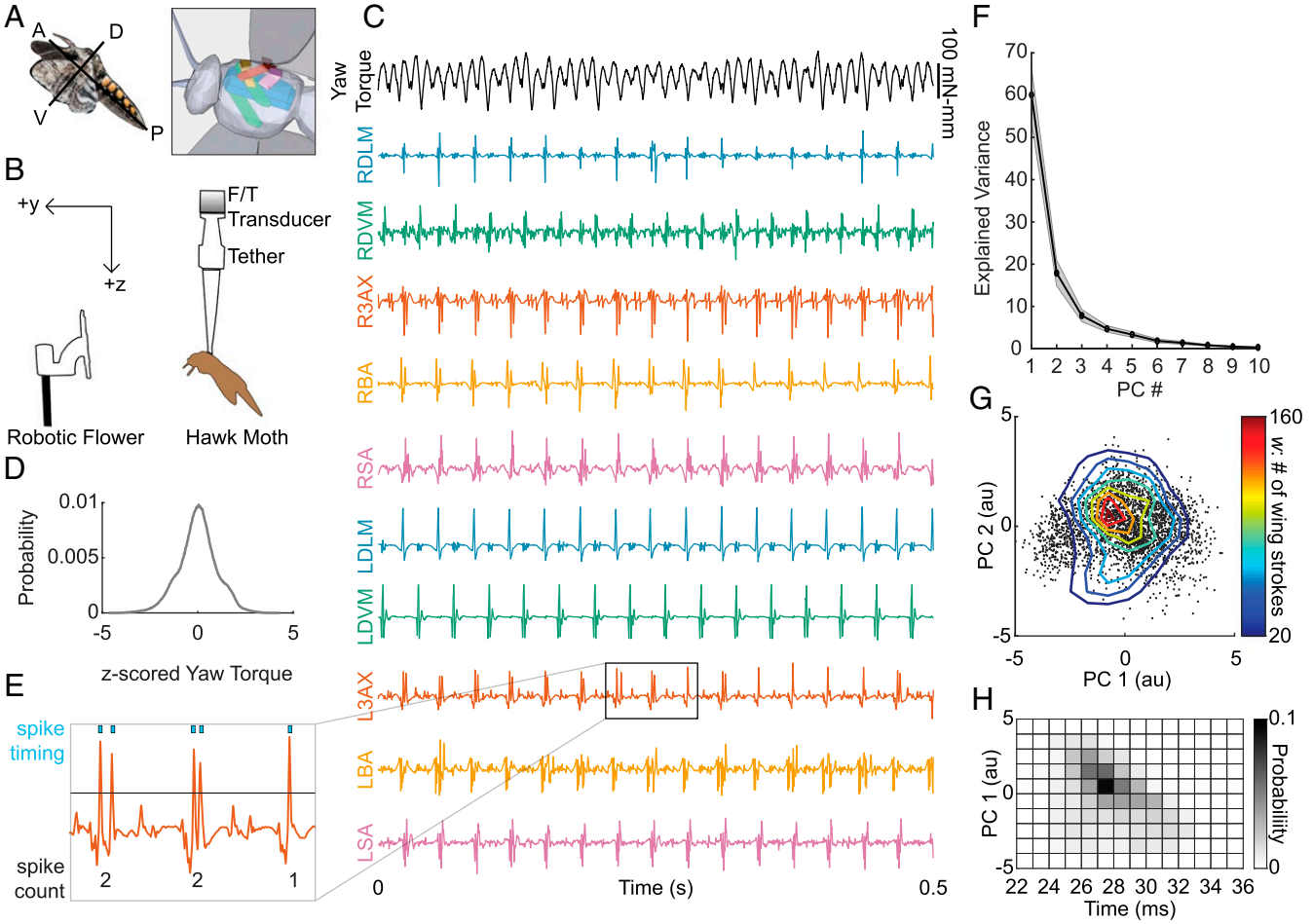

Fig. 1. EMGs from 10 flight muscles and simultaneous yaw torque. (*A*) A hawk moth, *M. sexta*, in flight, with a simplified 3D sketch of the 5 bilateral pairs of muscles from a ventrolateral view: dorsolongitudinal, DLM (blue); dorsoventral, DVM (green); third axillary, 3AX (orange); basalar, BA (yellow); and subalar, SA (purple). Muscles on the left and right sides of the animal are distinguished with an L or an R throughout the text (e.g., L3AX). (*B*) Hawk moths were presented a robotic flower oscillating with a 1-Hz sinusoidal trajectory while tethered to a custom 6-axis F/T transducer (N = 7 moths; 999 to 2,954 wing strokes per moth; average per moth = 1,950 wing strokes). (*C*) EMG and yaw torque (black) from 0.5 s of flight. (*D*) A histogram averaged across all moths of the raw yaw torque during shortened wing strokes z-scored (mean centered and scaled such that SD = 1) in each individual moth. The PCA was not done on z-scored data, and z scoring was only used here to make the scale of distributions comparable across moths. (*E*) Spike sorting was accomplished using threshold crossing (e.g., black line) in Offline Sorter (Plexon). Spike count is the number of spikes in each wing stroke, and spike timing is the precise spike time relative to the start of each wing stroke. (*F*) The first 2 PCs of the yaw torque waveforms captured most of the variance (mean, in black; ±SEM, in gray; N = 7 moths). (*G*) Projection of yaw torque onto the first 2 PCs for each wing stroke from a moth (w = 2,739 wing strokes) in PC space (arbitrary units, *au*). The joint histogram of the distribution is represented in a 10 × 10 grid between −5 and 5 using isoclines from the contour function in MATLAB (MathWorks). (*H*) Joint histogram of the scores of PC1 and the timing of the first RDVM spike in wing strokes in an example moth.

spike-resolved, comprehensive motor program, because all muscles actuating the wings are in the thorax and there are relatively few muscles compared to many segmented limbs. Moreover, flight muscles frequently function as single motor units because they are generally innervated by one, or very few, fast-type motor neurons with a 1:1 relationship between muscle and neural potentials (35, 36). A large number of spike-resolved motor units has been simultaneously recorded in locusts (37) and a smaller number simultaneously in flies and moths (38–40), although explicit analysis of encoding in count and timing has not been done in these systems. Invertebrate muscles have distinct count (number of spikes) and rate codes that do not have interchangeable effects on muscle force (19), but both of these are distinct from spike timing coding. Faster invertebrate muscles fire fewer times per cycle but can still show rate coding during and across wing strokes (29).

We take advantage of these features to capture a spike-resolved, comprehensive motor program in a hawk moth, *Manduca sexta*, and investigate the importance of spike timings in a nearly complete population code for movement. We examine how turning torque in every wing stroke is encoded by spike count (the number of spikes per wing stroke) and spike timing (the precise timing patterns of all spikes within each wing stroke) for each of the 10 muscles most important for controlling the wings (*SI Appendix*) (21, 41–43). This nearly complete motor program enables us to address 3 questions of ubiquity, consistency, and coordination in timing and count codes across this motor system.

Results

Temporal Information Is Ubiquitous in the Motor Program. We recorded a comprehensive motor program with spike-level resolution across all of the primary muscles actuating the wings in a hawk moth (*M. sexta*, $N = 7$) (Fig. 1*A*). The hawk moth musculature has been examined in detail anatomically and through in vivo and in vitro recordings (summarized in *SI Appendix*). Based on this rich literature, we identified 5 bilateral pairs of muscles that have important roles in controlling the wings during flight (*SI Appendix*, Fig. S1). We recorded EMG signals from these muscles while moths visually tracked a robotic flower in tethered, smooth pursuit flight (27, 44). We simultaneously recorded within-wing stroke yaw torque using a custom calibrated force–torque (FT) transducer (ATI Nano17Ti) (Fig. 1 *B* and *C*). The visual stimulus caused moths to generate variation in yaw torque (Fig. 1*D*). We segmented the EMG and torque data into wing strokes. We defined the onset time of each wing stroke as the zero phase crossing of the Hilbert transform of the moth's force in the z direction (45). The Hilbert transform estimates the instantaneous phase of a periodic signal. Here the zero phase crossing roughly corresponded to the peak downward force produced during each wing stroke. We treated each wing stroke as an independent sample of the muscle spikes and the yaw torque.

For the EMG data, we specified a time window relative to the onset of the wing stroke separately for each muscle to encompass the entire burst of spikes in all wing strokes. We computed the spike count (number of spikes per wing stroke) or the spike timing (precise spike times relative to the start of each wing stroke) for the 10 muscles (Fig. 1*E*). Because the wing stroke period varied a small amount (mean ± SD: 45.3 ± 3.8 ms across all moths), we shortened the yaw torque signal to the length of the shortest wing stroke for each moth. We also repeated our analyses with a phase code (timing normalized to wingstroke period) and obtained consistent results. We then found a lower-dimensional representation of the yaw torque using principal components analysis (PCA). The first 2 principal components (PCs) explained most of the variance (78.0 ± 10.6%) in yaw torque (Fig. 1*F*), so we represent the within-wing stroke yaw torque using the projection onto these first 2 PCs (the first 2 PC "scores"). The oscillating visual stimulus elicited variation in the moths' motor output and spiking activity (Fig. 1 *G* and *H*). The projection of yaw torque onto the first 2 PCs varies systematically with left and right turns and with straight flight (low asymmetry in yaw torque) in the middle decile (Fig. 2).

Both the spike count and the timing of spikes within the wing stroke show modulation along with the motor output (Fig. 3*A*). To test the contribution of spike timing encoding in individual muscles, we estimated the mutual information between muscle activity and yaw torque using the Kraskov k-nearest neighbors method, which is data-efficient and useful for experiments where sampling is finite and measured variables are continuous (46, 47). Unlike a direct method estimator, this method estimates mutual information between 2 variables (X and Y) using Euclidean distances between each sample (wing stroke) and its kth nearest neighbor in the space spanning the 2 variables of interest (for us, a representation of spiking activity and torque). The joint probability distribution of the distances and the number of samples within a neighborhood defined by these distances is used to estimate the joint entropy $H(X, Y)$ and the mutual information $I(X, Y)$ (*SI Appendix*, *SI Methods*).

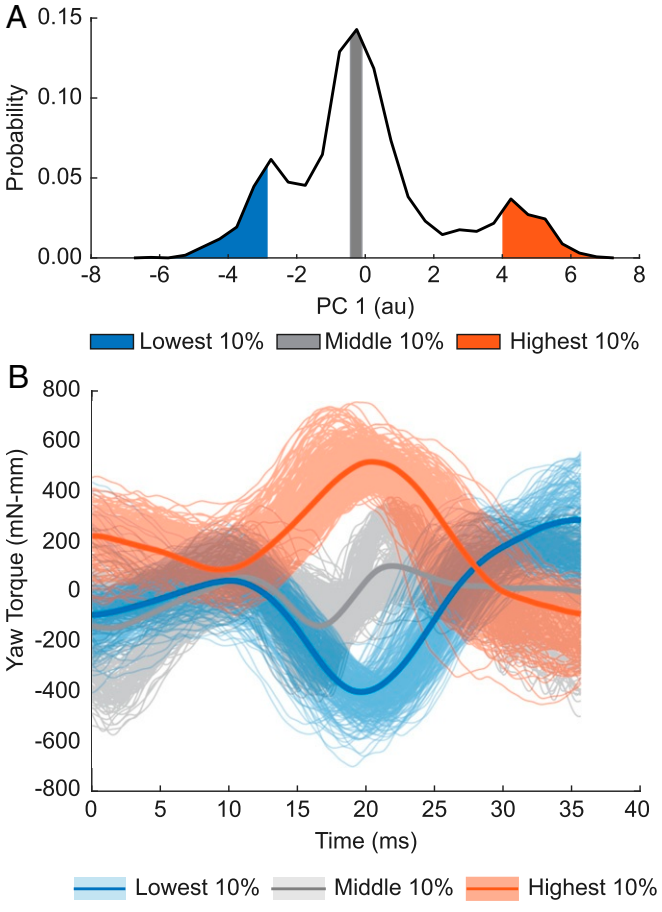

Fig. 2. Reconstructions using the first 2 PCs of yaw torque capture the main features of the raw torque waveforms. (*A*) Histogram of the scores of PC1 in an individual moth. The lowest decile (0 to 10%), the middle decile (45 to 55%), and highest decile (90 to 100%) are shaded in blue, gray, and orange, respectively. (*B*) The average reconstruction of wing strokes (solid lines) from the lowest (blue), middle (gray), and highest (orange) deciles using the dataset mean and the projections of scores onto the first 2 PCs, along with the raw torque waveforms (translucent lines) in each of these deciles. Deciles vary both in mean torque and the within-wing stroke torque waveforms consistent with previous results (45).

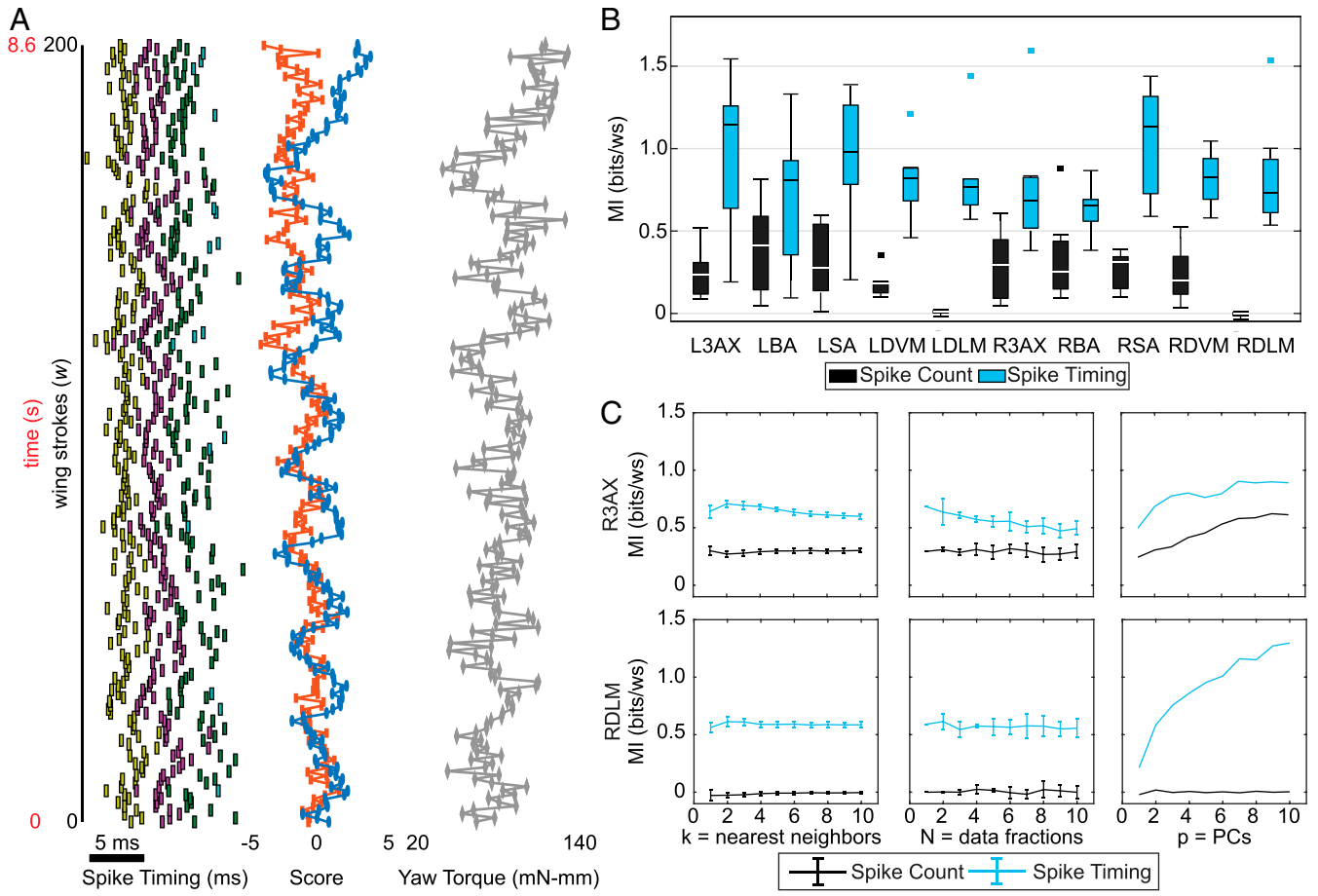

Fig. 3. Mutual information between spike count or spike timing and yaw torque. (*A*) Timing of spikes in the L3AX, the scores of the first 2 PCs, and the wing stroke average yaw torque show variability corresponding with the 1-Hz visual stimulus (200 wing strokes from a moth are shown). The rasters are the first (yellow), second (purple), third (green), and fourth (light blue) spikes within each wing stroke shown alongside the first (blue) and second (red) yaw torque PC scores and the raw yaw torque (gray). (*B*) MI estimates for spike count (black) and spike timing (blue) with yaw torque across individuals (N = 7). Box plots report the median as the center line in the box, which marks the 25th and 75th percentiles. Whiskers are the range of all points that are not considered outliers (square points). Spike count MI is less than spike timing MI (2-way ANOVA comparing timing vs. count for all muscles: count vs. timing, $P < 10^{-10}$; muscle ID, $P = 0.26$; interaction, $P = 0.09$). Spike timing MI is significantly greater than spike count MI in most paired comparisons within muscles (paired t tests: $P < 0.02$ for all muscles except the LBA, $P = 0.09$, and RBA, $P = 0.05$; Wilcoxon signed rank tests: $P < 0.02$ for all muscles except the LBA, $P = 0.11$, and RBA, $P = 0.08$). (*C*) MI estimates (mean $\pm$ SD) for the number of nearest neighbors k = 1 to 10, data fractions N = 1 to 10, and PCs included p = 1 to 10 from the RDLM and R3AX muscles of one moth (46, 47).

This information theoretic approach enables us to consider the importance of spike timing without assuming which features of the spike train are relevant or a linear relationship between spiking and motor output (48). It also enables separation of spike count mutual information (MI) from spike timing MI by conditioning spike timing on spike count (18),

$$I(S;\tau) = I(S_c;\tau) + \sum_{i=1}^{S_{c,max}} p(S_c = i) I(S_t;\tau \mid S_c = i), \qquad [1]$$

where S is the combined set of spike count and spike timings for each wingstroke, and τ is a vector of the projection of the yaw torque during the wingstroke onto the first 2 PCs. S_c is the spike count for each wing stroke taking discrete states, i, from 1 to $S_{c,max}$. Very small amplitude Gaussian noise with a SD of 10^{-4} was added to the discrete spike count variable so that it could be used in this continuous estimation method, as done previously (18). S_t is a vector of spike timings conditioned upon S_c such that, for each spike count, S_t has the same length, i. The first term is the mutual information between torque and count. The second term is the mutual information between torque and timing once the information in count is accounted for. All MI estimates reported in the main text use a value of $k = 4$.

For all 10 muscles, spike timing MI is higher than spike count MI (Fig. 3*B*). In all muscles, both mean spike count MI (range 0.0 to 0.4 bits per wing stroke [ws]) and mean spike timing MI (0.6 to 1 bits per ws) are nonzero, except for the DLM, which only spikes once per wing stroke during flight. Estimates of the spike count MI in the DLM are vanishingly small, but not exactly equal to 0 as would be expected with a constant spike count. This small nonzero bias was because of the added Gaussian noise to allow continuous MI estimation. All other muscles used a mixed encoding strategy, a combination of spike timing and spike count, to inform the torque. The error estimates of the MIs were small compared to the total MI (*SI Appendix*, Table S1; mean error < 0.04 bits per ws across all muscles). The MI estimates are stable across a range of k values (Fig. 3*C* and *SI Appendix*, Figs. S2 and S3). MI estimates can underestimate true MI given finite data; 90% of estimations from halved datasets deviated by less than 10% from the full dataset estimate, and our conclusions throughout the paper were robust to halving each dataset.

Temporal encoding is ubiquitous across the entire flight motor program, is present in every muscle, and is utilized more than count encoding (Fig. 3*B*). Each motor unit encodes almost more information per period about yaw torque in precise spike timings (0.8 bits per ws, on average, for all muscles) compared to other systems, like a cortical vocal area (between 0.1 and 0.3 bits per syllable) (25) and breathing muscles (between 0.05 and 0.2 bits per breath cycle) of song birds (18). The moth's 10 motor units code for flight using on the order of 1 bit per ws each.

Encoding Strategy Is Consistent across Functionally Diverse Muscles. Muscles in the hawk moth motor program have diverse biomechanical functions. For example, the main indirect downstroke muscle (DLM), acts by contracting the exoskeleton of the thorax, propagating mechanical strain to the wing hinge and indirectly causing the wings to depress (21). In contrast, the 3AX directly attaches to the wing hinge at the third axillary sclerite, which articulates the anal vein and remotes the wing (43, 49). Muscles also have variable spiking activity. Different muscles have different probability distributions of spike count per wing stroke (i.e., spike rate) and spike timing during the wing strokes (Fig. 4 *A* and *B*).

Despite their diverse properties, the 10 muscles in the motor program of the hawk moth are consistent in the magnitude and proportion of timing information used to encode yaw torque (Fig. 4*C*). No muscle conveys significantly different spike timing MI. Additionally, all muscles, other than the DLM, carry similar amounts of spike count MI. As a result, there is a consistent 3:1 ratio of spike timing MI to spike count MI for all muscles that spike more than once per wing stroke (Fig. 4 *C* and *E*: mean ± 95% CI of the mean of the ratio of spike timing MI to total MI excluding DLM = 0.75 ± 0.02).

Our conclusions were robust if we reduced the representation of the yaw torque to the scores of just the first PC (*SI Appendix*, Fig. S4*A*) or the average torque during a wing stroke (*SI Appendix*, Fig. S4*B*). Increasing dimension to 3 PCs (*SI Appendix*, Fig. S5) destabilizes estimates of information in some muscles, due to data limits, but our conclusions nonetheless remain consistent.

Neurons in some sensory systems may use distinct strategies to encode particular types of information (30). However, this is not the case in the hawk moth motor program. Even though each muscle has a different probability distribution of spike count and spike timing (Fig. 4 *A* and *B*), each muscle shares a comparable amount of MI with the moth's torque. The different

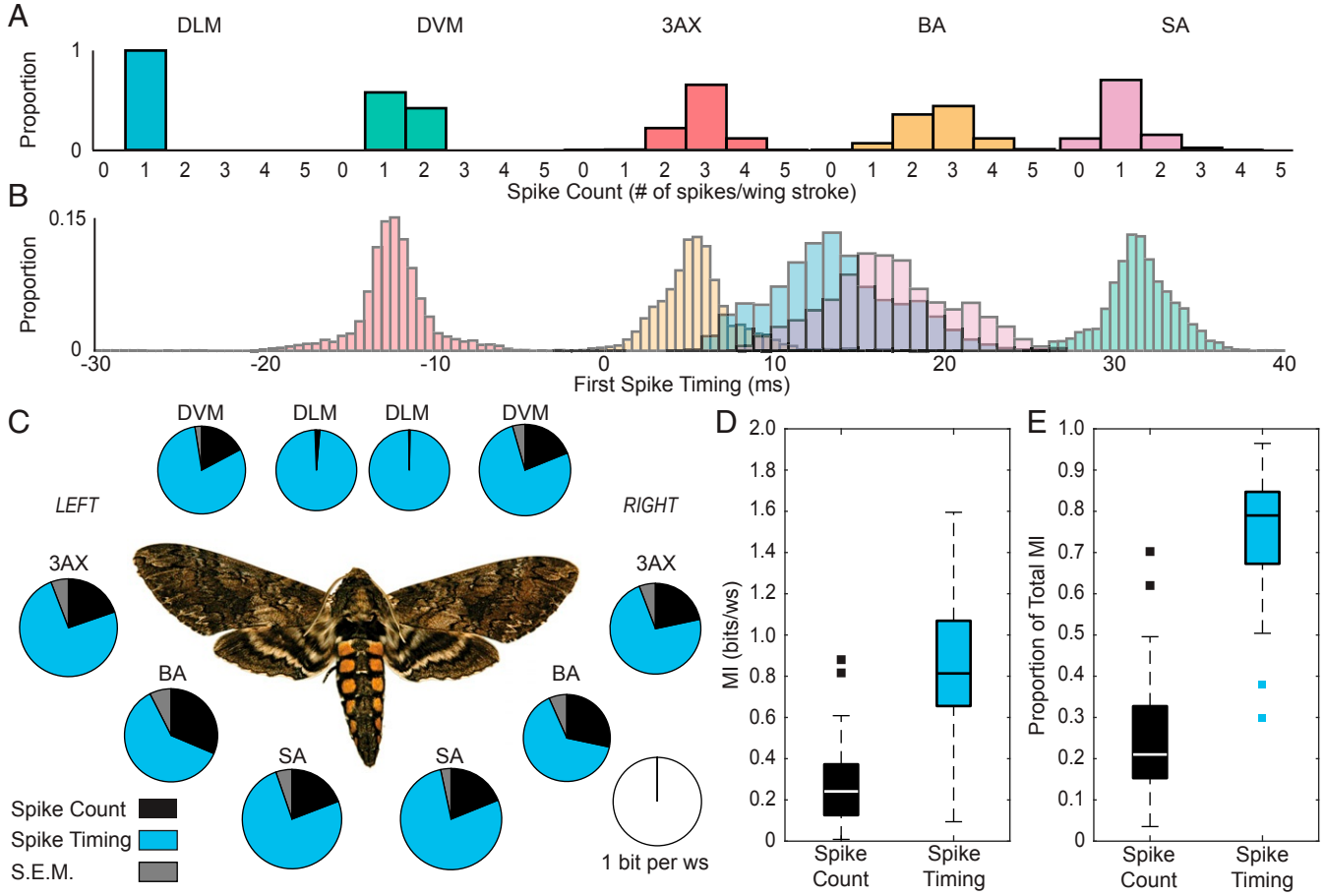

Fig. 4. Consistency of magnitude and proportion of spike timing MI and spike count MI in all 10 muscles. The 5 muscle types we recorded have different probability distributions of (*A*) spike count conditions and (*B*) the first spike timing (data shown for one moth). Some bursts begin before the wing stroke and continue into the wing stroke; these were reported as negative values ($t = 0$ corresponds to the start of the wing stroke). (*C*) Mean spike count and spike timing MI estimates for all 10 muscles across individuals ($N = 7$). Pie area indicates the magnitude of total MI, and the slices indicate the proportion that is spike count MI (black) and spike timing MI (blue), as well as the SEM of these proportions (gray). No significant difference was found in the magnitude of spike count MI of all muscles excluding the DLM (one-way ANOVA: $P = 0.66$; Kruskal–Wallis test: $P = 0.90$) or spike timing MI of all muscles (one-way ANOVA: $P = 0.54$; Kruskal–Wallis test: $P = 0.39$). No significant difference was found in the proportion of spike timing MI to total MI in all muscles excluding the DLM (one-way ANOVA: $P = 0.31$; Kruskal–Wallis test: $P = 0.54$). The (*D*) magnitude and (*E*) proportion of spike count MI (black) and spike timing MI (blue) across 8 muscles (DLM excluded) and 7 individuals. Boxplots display data as previously described in Fig. 3*B*.

probability distributions may indicate that different muscles have varying amounts of total entropy (bandwidth) while transmitting the same amount of information. Alternatively, different muscle types may have comparable total entropies but encode torque with varying precision.

Coordination Is Achieved through Timing, Not Count. Because timing is ubiquitous across all muscles and encoding strategies are consistent, we next investigated the role of spike timings in the coordination of multiple muscles. To do this, we first estimated the pairwise MI between the spiking activity of 2 muscles and the yaw torque,

$$I(S_A, S_B; \tau) = I([S_{A,c}\, S_{B,c}]; \tau) + \sum_{i_A=1}^{S_{A,c_{max}}} \sum_{i_B=1}^{S_{B,c_{max}}} p(i_A, i_B) I([S_{A,t}\, S_{B,t}]; \tau \mid (i_A, i_B)). \quad [2]$$

$I(S_A, S_B; \tau)$ is the pairwise MI, or the mutual information between the torque and the joint spiking activity of 2 muscles, S_A and S_B. As before (Eq. **1**), the first term is the pairwise spike count MI, and the second term is the pairwise spike timing MI. The estimates are weighted by the joint probability $p(i_A, i_B)$ of each possible pairwise spike count condition. As in the individual MI estimations, we used a value of $k = 4$ (*SI Appendix*, Fig. S6).

Then, we estimated the interaction information (II) between 2 muscles (50, 51),

$$II = I(S_A, S_B; \tau) - (I(S_A; \tau) + I(S_B; \tau)). \quad [3]$$

A positive II indicates net synergistic information, or that the muscles together reduce the entropy of the motor output more than the sum of their individual contributions. A negative II indicates that information is net redundant between the 2 muscles, or that there is coordination in the information content between the 2 muscles.

All pairwise combinations of muscles in the motor program have nonzero, negative II values (Eq. **3**), which are net redundant interactions (Fig. 5*A*). We separated the contributions of count and timing to II (*SI Appendix*, Eqs. **S1** and **S2**) and found that nearly all redundant information between muscles is

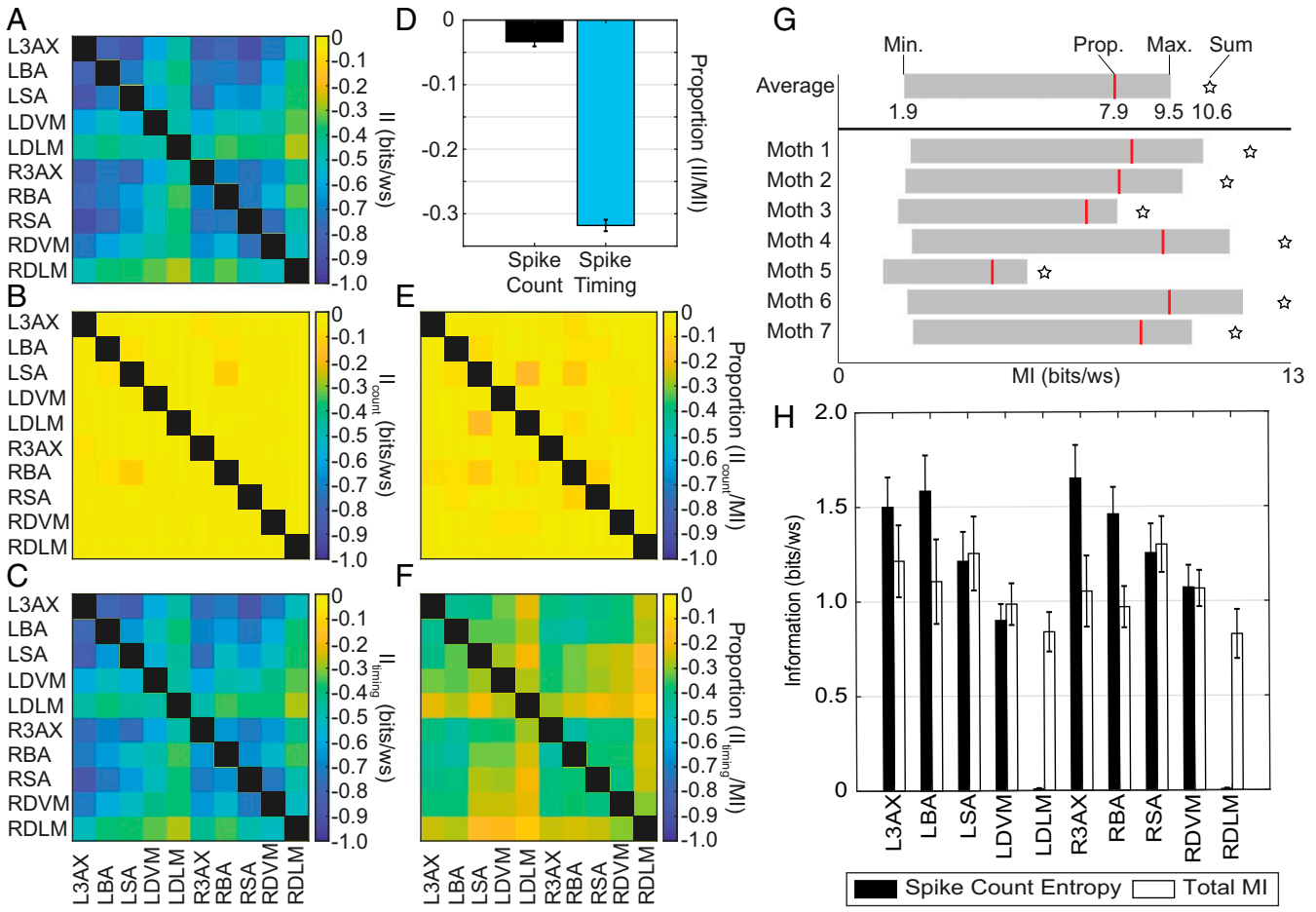

Fig. 5. Interaction information in pairwise combinations of muscles and the range of total motor program MI values possible. (*A*) We calculated total interaction information (*II*) (Eq. **3**) (50, 51) as a measure that compares the estimates of pairwise MI (Eq. **2**) and individual muscle MI (Eq. **1**) for all pairwise combinations of muscles (mean for $N = 7$ moths). All mean values of *II* are negative, indicating net redundant interactions or overlapping information content. Comparisons of muscles to themselves are excluded. (*B*) Spike count interaction information (II_{count}) and (*C*) spike timing interaction information (II_{timing}) across all pairwise combinations of muscles (*SI Appendix*, Eqs. **S1** and **S2**; mean for $N = 7$). (*D*) Proportion of *II* to the sum of individual muscle MIs for spike count (mean ± SEM for muscle pairs in all moths excluding DLMs, $n = 196$) and timing (mean ± SEM for muscle pairs in all moths including DLMs, $n = 315$) terms of *SI Appendix*, Eqs. **S1** and **S2**. (*E* and *F*) The proportion of (*E*) II_{count} and (*F*) II_{timing} to the sum of the individual spike count or timing MIs (mean for $N = 7$ individuals). (*G*) Estimates of lowest and highest values of total motor program MI (gray box), proportional estimate of motor program MI (red line), and sum of individual muscle MIs (star) for each moth and the population average. (*H*) Mean ± SEM of the spike count entropy (*SI Appendix*, Eq. **S3**) and the total MI ($N = 7$).

encoded in spike timing (Fig. 5 *B* and *C* and *SI Appendix*, Fig. S7). Mean spike count *II* is −0.023 ± 0.006 bits per ws, while mean spike timing *II* is −0.56 ± 0.04 bits per ws (±95% CI of the mean). Spike timing, not count, accomplishes essentially all of the coordination between muscles in the motor program. All conclusions were robust to halving the data size (*SI Appendix*, *SI Methods*).

It is possible that spike timing is more important for coordination than count simply because spike timing encodes more information overall. To test this, we scaled the spike count and spike timing interaction information according to the total magnitude of spike count and spike timing mutual information. Overall, 31.8 ± 0.9% of spike timing MI and 3.4 ± 0.9% of spike count MI in individual muscles is shared in pairwise interactions (Fig. 5*D*). Even considering the smaller magnitude of spike count MI in individual muscles, spike count encodes almost no coordinated information (Fig. 5 *E* and *F*). Count encoding of each muscle is independent of other muscles in the motor program.

The Motor Program Utilizes Less than 10 Bits per Wing Stroke. Coordination between muscles and limited amounts of information in each muscle suggest that the motor program operates with less than 10 bits of information per wing stroke. We created maximum, minimum, and intermediate estimates of the total information content of the motor program, using several methods to account for the redundant information in pairwise combinations (*SI Appendix*, Eqs. **S4** and **S5**). Because of sample size dependence in our individual and pairwise spike timing MI estimates, these values provide lower bounds on how much information could be encoded by the comprehensive motor program.

The comprehensive flight motor program uses an MI rate between 1.85 bits per ws and 9.47 bits per ws, with an intermediate estimate of 7.89 bits per ws (Fig. 5*G*). Since the average wing stroke length used in these calculations was 0.04 s, this corresponds to an information rate between 46.2 bits per s and 237 bits per s, or 4.6 to 23 bits per s per muscle. Lacking other comprehensive motor program recordings, it is difficult to compare information rates across motor systems. However, hawk moth flight is accomplished with a small information rate compared to those in sensory systems. While individual sensory neurons have comparable information rates [6 to 13 bits per s in RGCs (52) and 1 to 10 bits per s in olfactory receptors (53)], these systems have orders of magnitude more receptors, so the maximum information rate may be orders of magnitude higher overall [875,000 bits per s in the guinea pig retina (52)], although there is likely a great deal of redundancy in population codes.

Even an information rate of 7.89 bits per ws allows the moth to specify a large number of possible motor outputs. To estimate this range, we determined how many states in the empirical torque probability distribution could be encoded by the total motor program using the direct method (*SI Appendix*, Eq. **S6**). Given the intermediate estimate between the upper and lower values, the motor program MI can specify 483 ± 109 states of yaw torque ($N = 7$ individuals) for each wing stroke. We also estimated the entropy in spike count using the direct method (*SI Appendix*, Eq. **S3**). Excluding the DLM, the count entropy in each muscle was at least as large as the total MI (Fig. 5*H*). With noiseless transmission, the motor program could be encoded strictly in count.

Discussion

By investigating a comprehensive, spike-resolved motor program, we show that spike timing encoding is not a feature of just specialized motor units, but is a ubiquitous control strategy that is consistently used for activation and coordination of muscles. There are few, if any, differences in magnitudes and proportions of spike timing and spike count encoding between the various muscles controlling the wings (Figs. 3*B* and 4), despite their different modes of actuation and functional diversity (21). All muscles encode information about yaw torque in both precise spike timing and spike count (Fig. 4 *C*–*E*). Spike count is significant in every muscle with the exception of the DLMs, which only spike once per wing stroke during flight. However, when it comes to coordination between pairwise combinations of muscles, timing is almost everything.

The moth motor program has individual muscles acting as mixed spike timing and spike count encoders. In situ preparations of a wing elevator muscle in a locust, *Schistocerca nitens*, showed that changing either the spike timing or the number of spikes altered power output (54). Steering muscles, like the basalar muscle in the blowfly *Calliphora vicina*, can act by dissipating energy rather than doing positive work, and the timing of activation can modulate power (55). In this species, timing in the basalar muscle and coordination between pairs of activated muscles have been shown to affect wing kinematics and total body force (39, 40). Most mechanistic studies to date have examined how activation signals of a subset of muscles affect muscle force or body movements, but comprehensive stimulation investigating the effects of coordinated control mechanisms across muscles will be needed to understand functional implications. From our results, we now know that any studies of the moth's complete motor program must examine spike timing.

Spike timing can still matter in vertebrate muscle because of nonlinearity in force development and biomechanics (4). By shifting when in the strain cycle a muscle spikes, timing can modulate force as much as rate in animals from cockroaches (56) to turkeys (57). For example, the same spike triplet can result in different force production depending on whether it occurs at onset of or during tetanus (58). Pressure production in bird respiratory muscle is sensitive to spike timing down to the millisecond scale. Across all these cases, the complex transformation of motor unit spike patterns into force gives potential for precise timing to convey rich information to control movement. Spike timing codes with corresponding timing sensitivity in muscle power production may be a prevalent feature both in individual motor programs and across species.

Convergent Mixed Coding Strategies for Flight. An unexpected feature of the comprehensive motor program is the consistency in timing and count encoding across all of the motor units (Fig. 4). Calcium imaging of the direct muscles controlling the wings in *Drosophila* showed evidence for 2 categories of muscle encoding: phasic muscles that are transiently active, especially during saccades, or tonic muscles that are continuously active (23). Flies may utilize a dichotomy of these exclusively phasic and tonic muscles organized into mixed functional groups, where at least one phasic and one tonic muscle act on each sclerite. In contrast, *M. sexta* utilizes muscles with a mix of spike timing and spike count encoding. They usually have a larger, functionally dominant muscle (or muscles sharing innervation) in the group of muscles attached to sclerite as opposed to the similarly sized muscles attached to each sclerite in flies (*SI Appendix*). Additionally, *Drosophila* fly at wing beat frequencies an order of magnitude higher than *M. sexta* and *S. nitens*. Larger size and longer wingbeat periods might allow for a single mixed timing and count motor unit to have more power to control the sclerites. *M. sexta* also do not use saccades during flight, and muscles typically contract and relax on each cycle. While phasic and tonic calcium activation does not have the resolution of precise spiking activity, there is a separation of timescales and potential for separate mechanisms of muscle coordination.

The information framework we use here is powerful in its generality, separates timing and count, and reveals the ubiquity, consistency, and coordination of spike timing. However, it does not indicate content of the signals on its own. Many different parameters in the motor signals could covary with torque,

and dissecting each component will require other approaches. We complement this information approach by examining specific patterns of spike count and spike timing related to torque in 2 example moths (*SI Appendix*, Figs. S8 and S9). DLMs varied with turn direction, but in a narrow timing window with low variance. This is consistent with their known control potential where changing individual spike times by as little as ±4 ms can modulate the power output from 0% to 200% of normal and causally induce yaw torque (27). Overall, left and right pairs of muscles shifted their timing differences across turns. Time separation in the DVM and modulating of the timing of the 3AX were also consistent with earlier work (38, 59). There were also some individual differences, like in the basalar muscle where one moth increased the spike count for ipsilateral turns, while the other moth decreased the spike count. There may be significant individual variation in the particular control implementation each individual adopts even if the encoding strategy is conserved.

Spike Timing Codes Challenge Motor Circuit Precision. Timing codes are limited by precision, in the degree to which a spike can be both reliably specified by the nervous system and reliably translated by the muscle and skeletal machinery into differential forces (4). The precise spiking of the indirect flight muscles has causal consequences for turning down to the submillisecond scale (27). We now understand that this likely extends across the entire motor program (Fig. 3*B*) and that coordination is achieved primarily thorough spike timing across muscles (Fig. 5 *A*–*F*).

Given relatively few spikes per wing stroke, spike count per period could easily be interpreted as a rate code in fast, periodically activated muscles like the hawk moth flight musculature, but there is a distinction between rate and spike count in some slow muscles with many spikes per cycle. In the slow cycle frequencies of the crustacean stomastogastric pyloric rhythm and stick insect strides, muscle force does not strictly follow rate encoding and depends on the specific number of spikes (19, 20). Timing codes are also sometimes argued to be precise rate codes, but that would require drastic changes to spike rate in a very short time period for single spike codes, like the one present in the hawk moth DLM, and for codes that depend on specific spike patterns. For example, some slow muscles such as the radula closer in *Aplysia* show force dependence on specific patterns of spikes (60). Timing codes can be distinguished from rate or count codes by a specific pattern of spikes activated at a precise time in relation to a behavior (4). An alternative to a timing code is a phase code, although here they give similar results, because there is little variation in the wing beat period. It is possible that information in phase and absolute timing may differ in systems with more variation in the characteristic movement period.

It is still unknown how peripheral temporal codes arise from higher brain areas, the central nervous system, or motor circuits in the spinal or ventral nerve cord. Precise timing could come from direct connections between sensory receptors and efferent units. In moths, there are rapid mechanosensory pathways from the antenna (61), wings (62), and potentially other organs that can provide reafference of movement that could be used for precision. In locusts, mechanical feedback from the tegula, a sensory organ depressed during each wing stroke, produces phase resetting in the flight motor pattern which coordinates the fore and hind wings (63). In flies, gap junctions exist between precise haltere mechanoreceptors (64) and steering muscles (65), producing very fast reflexes. In conjunction with fast feedback from wing mechanoreceptors, these reflexes precisely pattern the activity of the first basalar muscle (66). However, these reflexes are still influenced by visual commands that incorporate feedback passing through a number of central nervous system synapses (67). The millisecond-scale resolution of the motor code poses a challenge even for neural processing that requires only a few synapses.

Precision may arise from central brain regions. Some pairs of bilateral muscles in *Drosophila* are innervated by motor neurons that receive input from the same circuitry in the nerve cord (68). This could give a proximal source of the left–right precision seen in *Manduca* downstroke muscles (27) but, alone, is unlikely to be sufficient to account for the prevalence of timing codes across all muscles. Peripheral precision may also come from transforming a population code or remapping of dynamics distributed over large populations of neurons (32). Both the central nervous system and rapid peripheral sensorimotor pathways provide potential mechanisms for spike timing precision.

Spike Count Does Not Inherently Limit Encoding. The prevalence of temporal coding in the moth motor program is not due to a limit on how much information can be encoded in spike count, since the spike count entropy was high enough to account for the total mutual information encoded by each muscle that spiked more than once per wing stroke (Fig. 5*H*). For the DVM and SA muscles, spike count would have to have no transmission error due to its entropy being similar in magnitude to the total MI, but, for the 3AX and BA muscles, there could be transmission error, and the spike count would still account for the total MI. Because much of the entropy in spike count is unused for encoding yaw torque, much of the variation in spike count must be ignored in the transformation from spiking activity to movement. This has precedence in cockroach running where muscle force in a limb muscle can be invariant to spike count (69). The opposing trends in BA spike count from our 2 example moths may not affect the yaw torque, because of this invariance (*SI Appendix*, Figs. S8 and S9).

While temporal codes are present in both faster, high-frequency systems and slower, low-frequency systems (18), count and rate codes are still used. Improved algorithms based on population rate codes for decoding motor implications of neural activity on a single-trial basis have led to better neural prosthetic devices and brain–machine interfaces (32, 70). Incorporating spike timing or pattern information could improve these devices by adding more information than what is present in just the rate code.

Spike Timing Is Essential to Coordination. The moth motor program has redundancy in its information transmission. Yet, our estimate of the motor program information rate, while accounting for shared information, still enables the encoding of hundreds of unique states. Redundancy and synergy in information transmission have been explored in the sensory periphery and in central brain regions where there may be a trade-off between code efficiency and robustness to noise (71–73). Dimensionality reduction techniques are commonly used to study populations of neurons in motor brain areas or ensembles of muscles (31, 32, 45, 70, 74–76). The activation patterns of many muscles may be represented by low-dimensional linear combinations of many muscles, "muscle synergies," that capture most of the variation (31, 45, 74, 75). There is potential confusion of the terms synergy and redundancy, because muscle synergies are likely to share net redundant (not synergistic) information. In the moth, all combinations of muscles do share information (negative II values).

Analysis without considering timing may miss important structure in how brains coordinate movement. Previous investigations of muscle synergies could not assess coordination at the spike level, although modulation of muscle activation over longer timescales was an important component of synergies identified in frogs, cats, and humans (33, 74, 76). In the *Manduca* system, nearly all of the coordination between muscles may be

overlooked by not considering spike timing. All muscles are more coordinated in their timings than the DLMs that have zero entropy in spike count. The spike timings of the DLM muscles have previously been shown to exhibit a low degree of coordination in their code for yaw torque (45). This is consistent with our results, since we found that these 2 muscles have the least pairwise interaction information (Fig. 5 *A*–*F* and *SI Appendix*, Fig. S6). Not all information encoded by individual muscles was shared. In the moth motor program, each muscle has a small amount of independent motor information it can convey with count, while control encoded in timing is coordinated across multiple muscles (Fig. 5*B*).

The hawk moth motor program uses a precise, coordinated spike timing code along with a less informative but independent spike count code consistently in every muscle used to control the wings. Spike timing codes likely necessitate millisecond-scale precision arising from either sensory feedback loops or central motor circuits. When combined with the growing number of specific examples of spike timing motor codes across vertebrates and invertebrates, the millisecond patterning of spikes cannot be safely ignored or necessarily relegated to a few specific cases. Timing encoding in the most peripheral motor output may be more of a rule, not an exception.

Materials and Methods

Data Archival. The data used in this paper are available on Dryad (https://doi.org/10.5061/dryad.r4xgxd280).

EMG Recordings from Flight Muscles. Moths (*M. sexta*) were obtained as pupae (University of Washington colony) and housed communally after eclosion with a 12-h light–dark cycle. Naïve males and females (N = 7) were used in experiments conducted during the dark period of their cycle. We cold-anesthetized moths before removing scales from the ventral and dorsal sides of their thoraxes. We made 2 small holes in the cuticle using insect pins and inserted 2 silver EMG wires to take differential recordings from the 10 indirect power muscles and direct steering muscles (*SI Appendix*, Fig. S1). These 5 pairs of muscles comprise a nearly complete motor program for flight (*SI Appendix*). A common ground wire was placed in the abdomen. We imaged the external placement of silver EMG wires to ensure we targeted the correct muscles (*SI Appendix*, Fig. S1). We also conducted postmortem dissections on a subset of animals to verify wire placement. All images were captured with a Zeiss Stereo Discovery v.12 equipped with a Zeiss Axiocam 105 color camera.

Experimental Setup. We tethered moths with cyanoacrylate glue to a 3-dimensional (3D)-printed acrylonitrile butadiene styrene (ABS) plastic rod rigidly attached to the F/T transducer (ATI Nano17Ti, FT20157; calibrated ranges: F_x, F_y = ±1.00 N; F_z = ±1.80 N; τ_x, τ_y, τ_z = ±6,250 mN·mm). After tethering, we allowed 30 min for the moths to adapt to dark light conditions and recover from the surgery at room temperature before starting experimental recordings. We amplified the EMG signals using a 16-channel alternating current (AC) amplifier (AM Systems Inc., Model 3500) before acquisition with an NI USB-6259 data acquisition (DAQ) board, which also sampled the F/T transducer (all sampling at 10,000 Hz). We captured outputs from these DAQ boards using MATLAB (MathWorks).

SI Appendix Methods. *SI Appendix* reports visual stimulus, spike train analysis, wing stroke alignment, and information theoretic estimates.

ACKNOWLEDGMENTS. We thank Mark Willis, Tom Daniel, Ilya Nemenman, and Sam Sober for helpful discussions. This material is based upon work supported by NSF Graduate Research Fellowships DGE-1650044 and DGE-1444932 and by an NSF Faculty Early Career Development Award (Award no. 1554790) to S.S. and a Klingenstein-Simons Fellowship in the Neurosciences to S.S.

1. S. P. Strong, R. Koberle, R. R. de Ruyter van Steveninck, W. Bialek, Entropy and information in neural spike trains. *Phys. Rev. Lett.* **80**, 197–200 (1998).
2. F. Theunissen, J. P. Miller, Temporal encoding in nervous systems: A rigorous definition. *J. Comput. Neurosci.* **2**, 149–162 (1995).
3. W. Gerstner, A. K. Kreiter, H. Markram, A. V. Herz, Neural codes: Firing rates and beyond. *Proc. Natl. Acad. Sci. U.S.A.* **94**, 12740–12741 (1997).
4. S. J. Sober, S. Sponberg, I. Nemenman, L. H. Ting, Millisecond spike timing codes for motor control. *Trends Neurosci.* **41**, 644–648 (2018).
5. J. T. Birmingham, Z. B. Szuts, L. F. Abbott, E. Marder. Encoding of muscle movement on two time scales by a sensory neuron that switches between spiking and bursting modes. *J. Neurophysiol.* **82**, 2786–2797 (1999).
6. R. C. deCharms, M. M. Merzenich, Primary cortical representation of sounds by the coordination of action-potential timing. *Nature* **381**, 610–613 (1996).
7. W. Bialek, F. Rieke, R. R. De Ruyter Van Steveninck, D. Warland. Reading a neural code. *Science* **252**, 1854–1857 (1991).
8. R. de Ruyter van Steveninck, W. Bialek, Real-time performance of a movement-sensitive neuron in the blowfly visual system: Coding and information transfer in short spike sequences. *Proc. R. Soc. Biol. Sci.* **234**, 379–414 (1988).
9. P. Reinagel, R. C. Reid, Temporal coding of visual information in the thalamus. *J. Neurosci.* **20**, 5392–5400 (2000).
10. E. L. Mackevicius, M. D. Best, H. P. Saal, S. J. Bensmaia, Millisecond precision spike timing shapes tactile perception. *J. Neurosci.* **32**, 15309–15317 (2012).
11. V. Lawhern, A. Nikonov, W. Wu, R. Contreras, Spike rate and spike timing contributions to coding taste quality information in rat periphery. *Front. Integr. Neurosci.* **5**, 1–14 (2011).
12. A. Egea-Weiss, A. Renner, C. J. Kleineidam, P. Szyszka, High precision of spike timing across olfactory receptor neurons allows rapid odor coding in *Drosophila*. *iScience* **4**, 76–83 (2018).
13. N. Brenner, S. P. Strong, R. Koberle, W. Bialek, R. R. d. R. van Steveninck, Synergy in a neural code. *Neural Comput.* **12**, 1531–1552 (2000).
14. E. Bülbring, Correlation between membrane potential, spike discharge, and tension in smooth muscle. *J. Physiol.* **128**, 200–221 (1955).
15. H. S. Milner-Brown, R. B. Stein, R. Yemm, Changes in firing rate of human motor units during linearly changing voluntary contractions. *J. Physiol.* **230**, 371–390 (1973).
16. D. Ferster, N. Spruston, Cracking the neuronal code. *Science* **270**, 756–757 (1995).
17. R. M. Enoka, J. Duchateau, Rate coding and the control of muscle force. *Cold Spring Harbor Perspect. Med.* **7**, a029702 (2017).
18. K. H. Srivastava *et al*.. Motor control by precisely timed spike patterns. *Proc. Natl. Acad. Sci. U.S.A.* **114**, 1171–1176 (2017).
19. L. G. Morris, S. L. Hooper, Muscle response to changing neuronal input in the lobster (*Panulirus interruptus*) stomatogastric system: Spike number- versus spike frequency-dependent domains. *J. Neurosci.* **17**, 5956–5671 (1997).
20. S. L. Hooper, C. Guschlbauer, G. von Uckermann, A. Büschges, Different motor neuron spike patterns produce contractions with very similar rises in graded slow muscles. *J. Neurophysiol.* **97**, 1428–1444 (2006).
21. A. E. Kammer, *Flying in Comprehensive Insect Physiology, Biochemistry and Pharmacology* (Pergamon Press, Oxford, United Kingdom, 1985).
22. M. Burrows, Flying, *The Neurobiology of an Insect Brain* (Oxford University Press, Oxford, United Kingdom, 1996), pp. 465–562.
23. T. Lindsay, A. Sustar, M. Dickinson, The function and organization of the motor system controlling flight maneuvers in flies. *Curr. Biol.* **27**, 345–358 (2017).
24. H. Ye, D. W. Morton, H. J. Chiel, Behavioral/systems/cognitive neuromechanics of multifunctionality during rejection in *Aplysia californica*. *J. Neurosci.* **26**, 10743–10755 (2006).
25. C. Tang, D. Chehayeb, K. Srivastava, I. Nemenman, S. J. Sober, Millisecond-scale motor encoding in a cortical vocal area. *PLoS Biol.* **12**, e1002018 (2014).
26. A. Suvrathan, H. L. Payne, J. L. Raymond, Timing rules for synaptic plasticity matched to behavioral function. *Neuron* **92**, 959–967 (2016).
27. S. Sponberg, T. L. Daniel, Abdicating power for control: A precision timing strategy to modulate function of flight power muscles. *Proc. R. Soc. Biol. Sci.* **279**, 3958–3966 (2012).
28. C. R. von Reyn *et al*., A spike-timing mechanism for action selection. *Nat. Neurosci.* **17**, 962–970 (2014).
29. M. H. Dickinson, M. S. Tu, The function of dipteran flight muscle. *Comp. Biochem. Physiol. Physiol.* **116**, 223–238 (1997).
30. M. Jamali, M. J. Chacron, K. E. Cullen, Self-motion evokes precise spike timing in the primate vestibular system. *Nat. Commun.* **7**, 1–14 (2016).
31. L. H. Ting, Dimensional reduction in sensorimotor systems: A framework for understanding muscle coordination of posture. *Prog. Brain Res.* **165**, 299–321 (2007).
32. M. M. Churchland *et al*., Neural population dynamics during reaching. *Nature* **487**, 1–20 (2012).
33. A. d'Avella, P. Saltiel, E. Bizzi, Combinations of muscle synergies in the construction of a natural motor behavior. *Nat. Neurosci.* **6**, 300–308 (2003).
34. Y. P. Ivanenko, R. E. Poppele, F. Lacquaniti, Five basic muscle activation patterns account for muscle activity during human locomotion. *J. Physiol.* **556**, 267–282 (2004).
35. P. N. R. Usherwood. The nature of 'slow' and 'fast' contractions in the coxal muscles of the cockroach. *J. Insect Physiol.* **8**, 31–52 (1962).
36. M. B. Rheuben, Quantitative comparison of the structural features of slow and fast neuromuscular junctions in *Manduca*. *J. Neurosci.* **5**, 1704–1716 (1985).
37. W. Zarnack, B. Möhl, Activity of the direct downstroke flight muscles of *Locusta migratoria* (L.) during steering behaviour in flight. *J. Comp. Physiol. A* **118**, 215–233 (1977).
38. H. Wang, N. Ando, R. Kanzaki, Active control of free flight manoeuvres in a hawkmoth, *Agrius convolvuli*. *J. Exp. Biol.* **211**, 423–432 (2008).
39. C. N. Balint, M. H. Dickinson, The correlation between wing kinematics and steering muscle activity in the blowfly *Calliphora vicina*. *J. Exp. Biol.* **204**, 4213–4226 (2001).
40. C. N. Balint, M. H. Dickinson, Neuromuscular control of aerodynamic forces and moments in the blowfly, *Calliphora vicina*. *J. Exp. Biol.* **207**, 3813–3838 (2004).

41. A. E. Kammer, The motor output during turning flight in a hawkmoth, *Manduca sexta*. *J. Insect Physiol.* **17**, 1073–1086 (1971).
42. A. E. Kammer, W. Nachtigall, Changing phase relationships among motor units during flight in a saturniid moth. *J. Comp. Physiol.* **83**, 17–24 (1973).
43. M. B. Rheuben, A. E. Kammer, Structure and innervation of the third axillary muscle of *Manduca* relative to its role in turning flight. *J. Exp. Biol.* **131**, 373–402 (1987).
44. S. Sponberg, J. P. Dyhr, R. W. Hall, T. L. Daniel, Luminance-dependent visual processing enables moth flight in low light. *Science* **348**, 1245–1248 (2015).
45. S. Sponberg, T. L. Daniel, A. L. Fairhall, Dual dimensionality reduction reveals independent encoding of motor features in a muscle synergy for insect flight control. *PLoS Comput. Biol.* **11**, 1–23 (2015).
46. A. Kraskov, H. Stögbauer, P. Grassberger, Estimating mutual information. *Phys. Rev. E* **69**, 066138 (2004).
47. C. M. Holmes, I. Nemenman, Estimation of mutual information for real-valued data with error bars and controlled bias. *Phys. Rev. E* **100**, 022404 (2019).
48. S. P. Strong, R. R. d. R. van Steveninck, W. Bialek, R. Koberle, On the application of information theory to neural spike trains. *Pac. Symp. Biocomput.* **3**, 621–632 (1998).
49. J. L. Eaton, *Lepidopteran Anatomy* (John Wiley, Hoboken, NJ, 1988).
50. N. Timme, W. Alford, B. Flecker, J. M. Beggs, Synergy, redundancy, and multivariate information measures: An experimentalist's perspective. *J. Comput. Neurosci.* **36**, 119–140 (2014).
51. R. A. A. Ince. Measuring multivariate redundant information with pointwise common change in surprisal. *Entropy* **19**, 318 (2017).
52. K. Koch *et al.*, How much the eye tells the brain. *Curr. Biol.* **16**, 1428–1434 (2006).
53. X. Z. N. Aldworth, X. M. A. Stopfer, Trade-off between information format and capacity in the olfactory system. *J. Neurosci.* **35**, 1521–1529 (2015).
54. A. P. Mizisin, R. K. Josephson, Mechanical power output of locust flight muscle. *J. Comp. Physiol. A* **160**, 413–419 (1987).
55. M. S. Tu, M. H. Dickinson, Modulation of negative work output from a steering muscle of the blowfly *Calliphora vicina*. *J. Exp. Biol.* **192**, 207–224 (1994).
56. S. Sponberg, A. J. Spence, C. H. Mullens, R. J. Full, A single muscle's multifunctional control potential of body dynamics for postural control and running. *Philos. Trans. R. Soc. Lond. Ser. B Biol. Sci.* **366**, 1592–1605 (2011).
57. T. J. Roberts, R. L. Marsh, P. G. Weyland, C. R. Taylor, Muscular force in running turkeys: The economy of minimizing work. *Science* **275**, 1113–1115 (1997).
58. F. Abbate, J. D. Bruton, A. De Haan, H. Westerblad, Prolonged force increase following a high-frequency burst is not due to a sustained elevation of Prolonged force increase following a high-frequency burst is not due to a sustained elevation of $[Ca^{2+}]_i$. *Am. J. Physiol. Cell Physiol.* **283**, C42–C47 (2002).
59. D. Springthorpe, M. J. Fernández, T. L. Hedrick, Neuromuscular control of free-flight yaw turns in the hawkmoth *Manduca sexta*. *J. Exp. Biol.* **215**, 1766–1774 (2012).
60. Y. Zhurov, V. Brezina, Variability of motor neuron spike timing maintains and shapes contractions of the accessory radula closer muscle of *Aplysia*. *J. Neurosci.* **26**, 7056–7070 (2006).
61. S. P. Sane, A. Dieudonné, M. A. Willis, T. L. Daniel, Antennal mechanosensors mediate flight control in moths. *Science* **315**, 863–866 (2007).
62. B. Pratt, T. Deora, T. Mohren, T. L. Daniel, Neural evidence supports a dual sensory-motor role for insect wings. *Proc. R. Soc. Biol. Sci.* **284**, 20170969 (2017).
63. H. Wolf, The locust tegula: Significance for flight rhythm generation, wing movement control and aerodynamic force production. *J. Exp. Biol.* **182**, 229–253 (1993).
64. J. L. Fox, A. L. Fairhall, T. L. Daniel, Encoding properties of haltere neurons enable motion feature detection in a biological gyroscope. *Proc. Natl. Acad. Sci. U.S.A.* **107**, 3840–3845 (2010).
65. A. Fayyazuddin, M. H. Dickinson, Haltere afferents provide direct, electrotonic Input to a steering motor neuron in the blowfly, *Calliphora*. *J. Neruosci.* **16**, 5225–5232 (1996).
66. A. Fayyazuddin, M. H. Dickinson, Convergent mechanosensory input structures the firing phase of a steering motor neuron in the blowfly, *Calliphora*. *J. Neurophysiol.* **82**, 1916–1926 (1999).
67. W. P. Chan, F. Prete, M. H. Dickinson, Visual input to the efferent control system of a fly's "gyroscope."*Science* **280**, 289–292 (1998).
68. S. Sadaf, O. V. Reddy, S. P. Sane, G. Hasan, Neural control of wing coordination in flies. *Curr. Biol.* **25**, 80–86 (2015).
69. S. Sponberg, R. J. Full, Neuromechanical response of musculo-skeletal structures in cockroaches during rapid running on rough terrain. *J. Exp. Biol.* **211**, 433–446 (2008).
70. C. Pandarinath *et al.*, Inferring single-trial neural population dynamics using sequential auto-encoders. *Nat. Methods* **15**, 805–815 (2018).
71. N. S. Narayanan, E. Y. Kimchi, M. Laubach, Redundancy and synergy of neuronal ensembles in motor cortex. *J. Neurosci.* **25**, 4207–4216 (2005).
72. J. L. Puchalla, E. Schneidman, R. A. Harris, M. J. Berry, Redundancy in the population code of the retina. *Neuron* **46**, 493–504 (2005).
73. D. S. Reich, F. Mechler, J. D. Victor, Independent and redundant information in nearby cortical neurons. *Science* **294**, 2566–2568 (2001).
74. L. H. Ting, J. M. Macpherson, A limited set of muscle synergies for force control during a postural task. *J. Neurophysiol.* **93**, 609–613 (2005).
75. G. Torres-Oviedo, L. H. Ting, Muscle synergies characterizing human postural responses. *J. Neurophysiol.* **98**, 2144–2156 (2007).
76. D. J. Clark, L. H. Ting, F. E. Zajac, R. R. Neptune, S. A. Kautz, Merging of healthy motor modules predicts reduced locomotor performance and muscle coordination complexity post-stroke. *J. Neurophysiol.* **103**, 844–857 (2009).